Mathematical Biosciences and Engineering

http://www.aimspress.com/journal/MBE

MBE, 23(3): 776–798.
DOI: 10.3934/mbe.2026030
Received: 25 November 2025
Revised: 22 January 2026
Accepted: 30 January 2026
Published: 06 February 2026

Research article

Impact of human behavior on the perpetuation of the *Echinococcus granulosus* life cycle: A mathematical approach

Richard Lagos[1,*], Andrei González-Galeano[2,3], Jaleydi Cárdenas-Poblador[4,5], Álvaro Mella-Parra[1] and María Esther Leyva-Borges[5]

[1] Departamento de Matemática y Física, Facultad de Ciencias, Universidad de Magallanes, Punta Arenas P.O. Box 113-D, Chile
[2] Centro de Ciencias Matemáticas, UNAM, Morelia, México
[3] Departamento de Matemáticas, Universidad El Bosque, Bogotá, Colombia
[4] Dynamical Systems Research Group, Departamento de Matemáticas y Física, Facultad de Ciencias Básicas e Ingeniería, Universidad de los Llanos, Villavicencio, Colombia
[5] Centro de Investigación en Matemáticas A.C., Guanajuato, México

* **Correspondence:** Email: richard.lagos@umag.cl.

Abstract: This study presents, as a proof-of-concept, a mathematical model describing the transmission dynamics of cystic echinococcosis. This neglected zoonosis is caused by the larval stage of *Echinococcus granulosus s.l.* involving dogs and sheep as definitive hosts and sheep as intermediate hosts. The model incorporates the dual role of humans as final hosts and as active participants in the parasite's transmission cycle through practices such as feeding dogs with infected viscera. A system of nine ordinary differential equations represents human subpopulations (children and adults) and the concentration of viable parasite eggs. The basic reproductive number (R_0) was computed via the next-generation matrix approach, and bifurcation analysis indicated a forward bifurcation at $R_0 = 1$, confirming that $R_0 < 1$ ensures disease control. Global sensitivity analysis using Sobol indices identified the infestation rate (β) and adult transmission rate (β_{AG}) as the most influential parameters, explaining 35.9% and 29.9% of R_0 variance, respectively. These findings highlight that interventions reducing β and β_{AG} may effectively decrease human infection rates.

Keywords: compartmental model; hydatidosis; neglected tropical disease; Sobol indices; zoonosis

1. Introduction

Cystic echinococcosis (CE), also known as hydatid disease, is a zoonosis caused by the larval stage of *Echinococcus granulosus sensu lato* (*E. granulosus s.l.*) [1–6]. The parasite's life cycle requires two

mammalian hosts: the dog (the definitive host), in which adult cestodes develop within the intestine, and the sheep (intermediate host), where hydatid cysts form in the viscera [7]. The domestic cycle begins when dogs ingest infected sheep viscera; the dogs subsequently expel eggs that contaminate pastures and water sources through their feces. Sheep then ingest these eggs while grazing, completing the cycle. CE remains endemic in sheep-farming regions, where specific socioeconomic practices sustain transmission despite ongoing control efforts.

The environmental presence of *E. granulosus s.l.* eggs in soil have not been fully utilized in mathematical models as an indicator of transmission dynamics to estimate prevalence in dogs and infection risk in sheep and humans. Environmental infestation, calculated as the percentage of positive samples per unit area

$$\frac{\#\text{ positive samples/area}}{\#\text{ samples analyzed/area}} \times 100$$

[8], directly reflects the contaminant load and its potential epidemiological impact [1–5, 9–11]. The persistence of echinococcosis in sheep production systems is influenced by human practices associated with slaughter and animal management, specifically the feeding of infected viscera to dogs. While studies have quantified environmental infestation through field and laboratory research, these have predominantly adopted a descriptive approach based on empirical data [2, 10, 11]. Humans assume a dual role in these epidemiological dynamics in that they act as 'victims' when infected and as 'perpetuating agents' through behaviors that sustain the parasite's cycle. Mathematical modeling, including both deterministic and stochastic variants, serves as a vital tool for identifying the fundamental parameters that govern disease transmission and spread [12–20]. Furthermore, it enables the evaluation of the potential impact of control measures not yet implemented in a target population. Existing literature reveals approaches that compartmentalize the three hosts into mutually exclusive groups based on the disease's natural history; some of these studies [17–19] incorporate the concentration of environmental eggs produced by infectious dogs.

In this paper, we propose a complementary mathematical modeling approach designed to explicitly represent the mechanisms sustaining disease perpetuation. This framework enables the analysis of diverse epidemiological scenarios contingent on environmental infestation levels and human behavior, providing a tool for a systemic understanding of the transmission process. To facilitate the modeling of individuals infected in childhood who remain asymptomatic until adulthood, the population is segmented into two age groups: children (under 15 years old) and adults. The resulting model consists of nine compartments: four for each age group, categorized by epidemiological status as susceptible, exposed, infected, or recovered, and an additional compartment representing the concentration of viable *E. granulosus s.l.* eggs in the environment. This methodology yields quantitative insights into the role of humans, which can be integrated into broader models of disease transmission and spread.

2. Materials and methods

2.1. The model

A mathematical model was developed to address the domestic life cycle of CE, identifying dogs as the definitive hosts and sheep as the intermediate hosts. Humans, categorized as either children (K) or adults (A), were incorporated as accidental hosts within the transmission cycle.

The human host populations were classified into standard epidemiological states: susceptible (s),

exposed (e), infected (i), and recovered (r). The variable X^k denotes the size of the host population $X \in \{K, A\}$ in the epidemiological class $k \in \{s, e, i, r\}$. Total population sizes were defined as $N^H = N^K + N^A$, where N^X represented the total size of host population X across all epidemiological classes.

The dynamics of CE transmission were formulated based on the variables and parameters defined in Tables 1 and 2, respectively. The model assumed that the susceptible child population K^s had a constant recruitment rate of μN. This population decreased upon exposure to the disease at a rate of β_{KG} or when maturing into susceptible adults A^s at a rate of τ. Conversely, K^s increased through the re-exposure of recovered children at a rate of m_1.

The population of exposed children (K^e) increased via interaction with an environment containing viable *E. granulosus s.l.* eggs (G) at a rate β_{KG}. This group decreased as individuals developed clinical symptoms at a rate of α_1, progressing to the infected stage K^i or maturing into exposed adults A^e at a rate of τ. Infected children K^i recovered at a rate of γ_1 or progressed to infected adult stage A^i at a rate of τ. A natural death rate, d, was applied to all human compartments.

For the adult population, A^s increased through the re-exposure of recovered individuals at a rate of m_2 and decreased upon exposure at a rate of β_{AG}. Exposed adults (A^e) increased through environmental interaction at a rate of β_{AG} and decreased at a rate of α_2 upon showing symptoms, progressing to A^i, who subsequently recovered at a rate of γ_2.

In practice, CE prevalence in dogs was determined through parasitological fecal diagnosis using the enzyme-linked immunosorbent assay (ELISA), DNA detection, or polymerase chain reaction (PCR). These assessments were conducted within epidemiological units that accounted for local risk factors such as slaughtering practices and viscera disposal methods. The results were used to calculate the environmental infestation index (EII), defined as [8]

$$EII = \frac{\text{Number of positive samples/area}}{\text{Number of samples analyzed/area}} \times 100.$$

Assuming regular EII measurements within fixed areas, this metric was introduced into the mathematical model as the environmental infestation rate, denoted by β.

It was further assumed that exposed and infected adults maintained the parasite cycle by feeding dogs with parasitized viscera at a rate of β. These assumptions provided the framework for analyzing the interaction between the parasite cycle and human disease dynamics (see Figure 1). Consequently, the transmission dynamics of CE in human populations were expressed by the following system of ordinary differential equations.

The model proposed the hypothesis that, under specific conditions, the concentration of viable *E. granulosus s.l.* eggs was influenced by the infestation rate β. Specifically, it was postulated that in cases where $b = d_G$, the parameter β played a critical role in increasing the concentration of the causative agent in the human population.

$$
\begin{aligned}
\frac{dK^s}{dt} &= \mu N + m_1 K^r - (d + \tau + \beta_{KG} G/N)\, K^s,\\
\frac{dK^e}{dt} &= \beta_{KG} G K^s/N - (d + \tau + \alpha_1)\, K^e,\\
\frac{dK^i}{dt} &= \alpha_1 K^e - (d + \tau + \gamma_1)\, K^i,\\
\frac{dK^r}{dt} &= \gamma_1 K^i - (d + \tau + m_1)\, K^r,\\
\frac{dA^s}{dt} &= \tau K^s + m_2 A^r - (d + \beta_{AG} G/N)\, A^s,\\
\frac{dA^e}{dt} &= \tau K^e + \beta_{AG} G A^s/N - (d + \alpha_2)\, A^e,\\
\frac{dA^i}{dt} &= \tau K^i + \alpha_2 A^e - (d + \gamma_2)\, A^i,\\
\frac{dA^r}{dt} &= \tau K^r + \gamma_2 A^i - (d + m_2)\, A^r,\\
\frac{dG}{dt} &= (b - d_G)G + \frac{\beta}{N}\left(A^e + A^i\right).
\end{aligned}
\tag{2.1}
$$

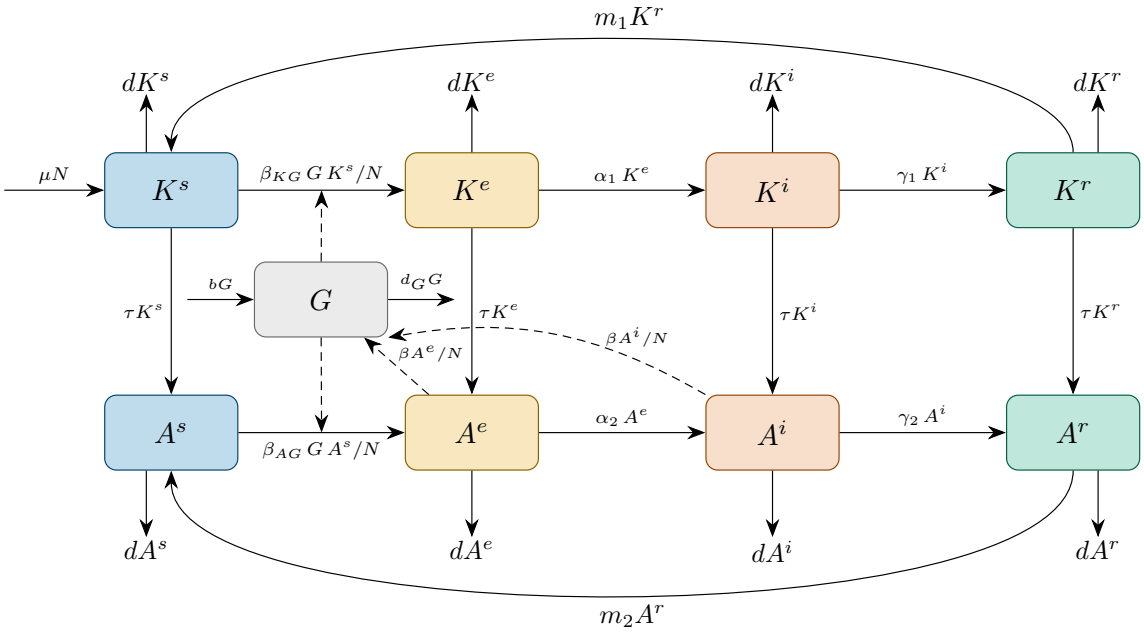

Figure 1. Flowchart for the model of human population epidemiological stage compartments.

2.2. *Well-posedness of the solutions*

To ensure the model (2.1) was epidemiologically and mathematically well-posed, its properties

were verified within a feasible domain prior to the primary mathematical analysis.

Theorem 1. *The nonnegative orthant*

$$\mathcal{M} = \left\{ \boldsymbol{x} = \left(K^s, K^e, K^i, K^r, A^s, A^e, A^i, A^r, G \right) \in \mathbb{R}^9_+ \right\} \tag{2.2}$$

is a positively invariant set for system (2.1). *Consequently, all solutions of the system remain nonnegative for nonnegative initial data.*

Proof. Observe that each component equation of system (2.1) can be written in the form

$$\frac{dx_i}{dt} = f_i(\boldsymbol{x}) = g_i(\boldsymbol{x}) - h_i(\boldsymbol{x})\, x_i, \tag{2.3}$$

where $x_i \in \{K^s, K^e, K^i, K^r, A^s, A^e, A^i, A^r, G\}$.

Moreover, each function $g_i(\boldsymbol{x})$ does not explicitly depend on x_i and satisfies $g_i(\boldsymbol{x}) \geq 0$ whenever $x_j \geq 0$ for all $j \neq i$. Therefore, for each i,

$$\left.\frac{dx_i}{dt}\right|_{x_i=0} = f_i(\boldsymbol{x})|_{x_i=0} \geq 0, \qquad \text{whenever } x_j \geq 0 \text{ for all } j \neq i. \tag{2.4}$$

This implies that the vector field points inward on the boundary of $\mathcal{M}$, and so $\mathcal{M}$ is a positively invariant set for system (2.1).

2.3. Disease-free equilibrium and calculation of the basic reproductive number

The basic reproductive number (R_0) was identified as a critical parameter within the mathematical modeling of infectious diseases. This value represents the average number of secondary infections generated by a single infectious individual introduced into a completely susceptible population. Its value determines the potential for disease persistence: If $R_0 < 1$, the infection tends toward extinction, whereas if $R_0 > 1$, the disease may persist and spread within the population [21].

This study implemented the approach proposed by van den Driessche [22] to calculate R_0. This method, based on decomposing the system into *new infections* and *transitions* between compartments, utilized the *next-generation matrix* to provide a robust framework for compartmental models.

To compute R_0, the next-generation matrix approach was employed. Let $x \in \mathbb{R}^m$ denote the vector of infected (or infection-related) compartments, those containing individuals capable of contributing to new infections. The dynamics of the infected subsystem were expressed as

$$\dot{\mathbf{x}} = \mathcal{F}(x) - \mathcal{V}(x),$$

where $\mathcal{F}$ represents the rate of appearance of new infections that appear in each compartment, and $\mathcal{V}$ accounts for all other transitions, including disease progression, recovery, natural death, and movement between infected classes. For the proposed model, the vectors $\mathcal{F}$ and $\mathcal{V}$ were defined based on the interaction rates between human hosts and the environment.

$$\mathcal{F} = \begin{pmatrix} \frac{\beta_{KG} G}{N} K^S \\ 0 \\ \frac{\beta_{AG} G}{N} A^S \\ 0 \\ bG + \frac{\beta}{N}(A^e + A^i) \end{pmatrix} \mathcal{V} = \begin{pmatrix} (d + \tau + \alpha_1) K^e \\ -\alpha_1 K^e + (d + \tau + \gamma_1) K^i \\ -\tau K^e + (d + \alpha_2) A^e \\ -\tau K^i - \alpha_2 A^e + (d + \gamma_2) A^i \\ d_G G \end{pmatrix}. \tag{2.5}$$

The model was then evaluated at the disease-free equilibrium (DFE),

$$E_0 = (K_0^s, K_0^e, K_0^i, K_0^r, A_0^s, A_0^e, A_0^i, A_0^r, G_0),$$

where

$$\begin{aligned} K_0^s &= \frac{\mu N}{d+\tau}, \\ A_0^s &= \frac{\tau}{d} K_0^s = \frac{\tau \mu N}{d(d+\tau)}, \\ K_0^e &= K_0^i = K_0^r = A_0^e = A_0^i = A_0^r = G_0 = 0. \end{aligned} \tag{2.6}$$

The DFE was obtained by setting all infected compartments to zero and solving the remaining steady-state equations for the susceptible populations. Subsequently, the Jacobian matrices of $\mathcal{F}$ and $\mathcal{V}$ were computed with respect to the infected variables at the DFE, denoted as F and V, respectively:

$$F = \frac{\partial \mathcal{F}}{\partial x}\Big|_{E_0}, \qquad V = \frac{\partial \mathcal{V}}{\partial x}\Big|_{E_0}.$$

In this case,

$$F = \begin{pmatrix} 0 & 0 & 0 & 0 & \frac{\beta_{KG}}{N} K_0^S \\ 0 & 0 & 0 & 0 & 0 \\ 0 & 0 & 0 & 0 & \frac{\beta_{AG}}{N} A_0^S \\ 0 & 0 & 0 & 0 & 0 \\ 0 & 0 & \frac{\beta}{N} & \frac{\beta}{N} & b \end{pmatrix},$$

$$V = \begin{pmatrix} (d+\tau+\alpha_1) & 0 & 0 & 0 & 0 \\ -\alpha_1 & (d+\tau+\gamma_1) & 0 & 0 & 0 \\ -\tau & 0 & (d+\alpha_2) & 0 & 0 \\ 0 & -\tau & -\alpha_2 & (d+\gamma_2) & 0 \\ 0 & 0 & 0 & 0 & d_G \end{pmatrix}, \tag{2.7}$$

$$V^{-1} = \begin{pmatrix} \frac{1}{(d+\tau+\alpha_1)} & 0 & 0 & 0 & 0 \\ \frac{\alpha_1}{(d+\tau+\alpha_1)(d+\tau+\gamma_1)} & \frac{1}{(d+\tau+\gamma_1)} & 0 & 0 & 0 \\ \frac{\tau}{(d+\tau+\alpha_1)(d+\alpha_2)} & 0 & \frac{1}{(d+\alpha_2)} & 0 & 0 \\ \frac{\tau\alpha_1}{(d+\tau+\alpha_1)(d+\tau+\gamma_1)(d+\gamma_2)} + \frac{\tau\alpha_2}{(d+\tau+\alpha_1)(d+\alpha_2)(d+\gamma_2)} & \frac{\tau}{(d+\tau+\gamma_1)(d+\gamma_2)} & \frac{\alpha_2}{(d+\alpha_2)(d+\gamma_2)} & \frac{1}{(d+\gamma_2)} & 0 \\ 0 & 0 & 0 & 0 & \frac{1}{d_G} \end{pmatrix}.$$

The next-generation matrix was then defined as

$$K = FV^{-1}.$$

The basic reproductive number was computed as the spectral radius (the largest nonnegative eigenvalue) of this matrix:

$$R_0 = \rho(FV^{-1}).$$

Consequently, the basic reproductive number for the mathematical model (2.1) was determined to be

$$\begin{aligned} R_0 = & \sqrt{\frac{bA_0^s\alpha_2\beta\beta_{AG}}{N^2(\alpha_2+d)(d+\gamma_2)d_G}} \\ & + \frac{bA_0^s\beta\beta_{AG}}{N^2(\alpha_2+d)d_G} \\ & + \frac{b\alpha_1\beta\beta_{KG}K_0^s\tau}{N^2(d+\gamma_2)(\alpha_1+d+\tau)(d+\gamma_1+\tau)d_G} \\ & + \frac{b\alpha_2\beta\beta_{KG}K_0^s\tau}{N^2(\alpha_2+d)(d+\gamma_2)(\alpha_1+d+\tau)d_G} \\ & + \frac{b\beta\beta_{KG}K_0^s\tau}{N^2(\alpha_2+d)(\alpha_1+d+\tau)d_G}. \end{aligned} \tag{2.8}$$

The resulting R_0 for the mathematical model (2.1) represents the threshold for domestic transmission dynamics. The following theorem establishes the fundamental property of R_0 as a threshold value at $R_0 = 1$, which follows directly from the construction of the next-generation matrix.

Theorem 2. *Given the model (2.1), the disease-free equilibrium E_0 is locally asymptotically stable if and only if $R_0 < 1$.*

Proof. See [22].

2.4. Equilibrium points

2.4.1. Case $b = d_G$

Theorem 3. *If $b = d_G$, the disease-free equilibrium is the unique equilibrium of system* (2.1).

Proof. Assume equilibrium conditions and let $b = d_G$. Then, from the equation governing G, it follows that

$$\frac{\beta}{N}\left(A^e + A^i\right) = 0.$$

By the positivity of solutions, this implies $A^e = A^i = 0$. Substituting these values into the equilibrium equations for A^i, K^i, K^r, and A^r yields

$$K^i = K^e = K^r = A^r = 0.$$

Next, the equilibrium equation for A^e reduces to $GA^s = 0$. If $A^s = 0$, then substituting all equilibrium values into the equations for A^s and K^s leads to $\mu N = 0$, a contradiction. Hence, $G = 0$, and consequently,

$$K^s = \frac{\mu N}{d+\tau}, \qquad A^s = \frac{\tau\mu N}{d(d+\tau)}.$$

Thus, the unique equilibrium point is

$$\boldsymbol{x}^* = \left(\frac{\mu N}{d+\tau}, 0, 0, 0, \frac{\tau\mu N}{d(d+\tau)}, 0, 0, 0, 0\right), \tag{2.9}$$

which corresponds to the disease-free equilibrium.

2.4.2. General case

We consider system (2.1) at equilibrium by blocks: first the children block, then the adult block, and finally the parasites block. Our goal is to characterize a general equilibrium with components

$$(K_s^*, K_e^*, K_i^*, K_r^*, A_s^*, A_e^*, A_i^*, A_r^*, G^*)\,.$$

(I) Children block

From the differential equations associated with K^e, K^i, and K^r, it follows that

$$K_e^* = A_1 G^* K_s^*, \quad \text{where } A_1 = \frac{\beta_{KG}/N}{d+\tau+\alpha_1}, \tag{2.10}$$

$$K_i^* = A_2 K_e^* = A_2 A_1 G^* K_s^*, \quad \text{where } A_2 = \frac{\alpha_1}{d+\tau+\gamma_1}, \tag{2.11}$$

$$K_r^* = A_3 K_i^* = A_3 A_2 A_1 G^* K_s^*, \quad \text{where } A_3 = \frac{\gamma_1}{d+\tau+m_1}. \tag{2.12}$$

Hence,

$$K_s^* + K_e^* + K_i^* + K_r^* = K_s^* + A G^* K_s^*, \tag{2.13}$$

where $A = A_1 + A_1A_2 + A_1A_2A_3$.

Let $K = K^s + K^e + K^i + K^r$. Then,

$$\frac{dK}{dt} = \frac{dK^s}{dt} + \frac{dK^e}{dt} + \frac{dK^i}{dt} + \frac{dK^r}{dt} = -(d+\tau)K + \mu N. \tag{2.14}$$

At equilibrium, $\dfrac{dK}{dt} = 0$, and therefore,

$$K^* = \frac{\mu N}{d+\tau}, \tag{2.15}$$

which implies

$$K_s^* + K_e^* + K_i^* + K_r^* = \frac{\mu N}{d+\tau}.$$

Combining this relation with (2.13), we obtain

$$K_s^* + A G^* K_s^* = \frac{\mu N}{d+\tau}. \tag{2.16}$$

(II) Adults block

From the differential equations associated with A^e, A^i, and A^r, we obtain

$$A_e^* = B_1 K_e^* + B_2 G^* A_s^*, \quad \text{where } B_1 = \frac{\tau}{d+\alpha_2}, \;\; B_2 = \frac{\beta_{AG}/N}{d+\alpha_2}, \tag{2.17}$$

$$A_i^* = B_3 K_i^* + B_4 A_e^*, \quad \text{where } B_3 = \frac{\tau}{d+\gamma_2}, \;\; B_4 = \frac{\alpha_2}{d+\gamma_2}, \tag{2.18}$$

$$A_r^* = B_5 K_r^* + B_6 A_i^*, \quad \text{where } B_5 = \frac{\tau}{d+m_2}, \;\; B_6 = \frac{\gamma_2}{d+m_2}. \tag{2.19}$$

Consequently,

$$A_s^* + A_e^* + A_i^* + A_r^* = A_s^* + CG^*A_s^* + BG^*K_s^*, \tag{2.20}$$

where $B = A_1B_1 + A_1A_2B_3 + A_1B_1B_4 + A_1A_2A_3B_5 + A_1A_2B_3B_6 + A_1B_1B_4B_6$, $C = B_2 + B_2B_4 + B_2B_4B_6$.

Let $A = A^s + A^e + A^i + A^r$. Then,

$$\frac{dA}{dt} = \frac{dA^s}{dt} + \frac{dA^e}{dt} + \frac{dA^i}{dt} + \frac{dA^r}{dt} = \tau K - dA. \tag{2.21}$$

At equilibrium, $\dfrac{dA}{dt} = 0$, yielding

$$A^* = \frac{\tau}{d}K^* = \frac{\tau\mu N}{d(d+\tau)}. \tag{2.22}$$

Thus,

$$A_s^* + A_e^* + A_i^* + A_r^* = \frac{\tau\mu N}{d(d+\tau)}.$$

Combining this relation with (2.20), we obtain

$$A_s^* + CG^*A_s^* + BG^*K_s^* = \frac{\tau\mu N}{d(d+\tau)}. \tag{2.23}$$

(III) Parasites block

At equilibrium, the parasites equation yields

$$G^* = \frac{\beta/N}{d_G - b}\left(A_e^* + A_i^*\right), \tag{2.24}$$

provided that $d_G - b \neq 0$. Recall that the case $d_G = b$ has already been analyzed.

Using expressions (2.17) and (2.18) for A_e^* and A_i^*, respectively, we obtain

$$G^* = DG^*\left(EK_s^* + FA_s^*\right), \tag{2.25}$$

where $D = \dfrac{\beta/N}{d_G - b}$, $E = A_1B_1 + A_1A_2B_3 + A_1B_1B_4$, $F = B_2 + B_2B_4$.

Our objective is now to analyze the solutions of the system (2.16)–(2.23)–(2.25) for K_s^*, A_s^*, and G^*, treating A, B, C, D, E, and F as previously defined constants.

Equation (2.25) can be rewritten as

$$G^*\left[1 - D\left(EK_s^* + FA_s^*\right)\right] = 0. \tag{2.26}$$

If $G^* = 0$, then

$$(K_s^*, K_e^*, K_i^*, K_r^*, A_s^*, A_e^*, A_i^*, A_r^*, G^*) = \left(\frac{\mu N}{d+\tau}, 0, 0, 0, \frac{\tau\mu N}{d(d+\tau)}, 0, 0, 0, 0\right), \tag{2.27}$$

which corresponds to the disease-free equilibrium.

If $1 - D\left(EK_s^* + FA_s^*\right) = 0$, then

$$EK_s^* + FA_s^* = \frac{1}{D}. \tag{2.28}$$

From (2.16) and (2.23), respectively, we obtain

$$K_s^* = \frac{I}{1 + AG^*}, \qquad A_s^* = \frac{H(1 + AG^*) - BIG^*}{(1 + AG^*)(1 + CG^*)}, \tag{2.29}$$

where $H = \dfrac{\tau\mu N}{d(d+\tau)}$, $I = \dfrac{\mu N}{d+\tau}$.

Substituting into (2.28), we obtain a quadratic equation for G^*:

$$\frac{AC}{D}(G^*)^2 + \left(\frac{A+C}{D} - EIC - AFH - BFI\right)G^* - \left(EI + FH - \frac{1}{D}\right) = 0. \tag{2.30}$$

Once G^* is determined, the values of K_s^* and A_s^* follow from (2.29), and the remaining equilibrium components can be computed iteratively.

2.5. Model bifurcation

Once the value of R_0 has been determined, the following step in the process is to analyze the dynamics of the system around the critical threshold $R_0 = 1$. In this context, bifurcation theory plays a crucial role, as it allows for the description of the changes in the endemic equilibrium as the parameters are altered around this threshold. In particular, by applying the center manifold theorem developed by Castillo Chávez [25], it is possible to determine the direction of the bifurcation and establish whether the model exhibits a forward or backward bifurcation.

From an epidemiological perspective, this analysis is highly relevant. In models demonstrating forward bifurcation, the design of control strategies that reduce R_0 to 1 is sufficient to achieve disease eradication. However, in the presence of backward bifurcation, even when $R_0 < 1$, the infection can persist, implying the need to implement stricter control measures to completely eliminate the disease [23–25].

The present study shows that the model under analysis exhibits a forward bifurcation, implying that the condition $R_0 = 1$ is sufficient to control the spread of the disease. The findings obtained from this study contribute to a more profound comprehension of transmission thresholds and furnish a robust mathematical framework for the design of effective control strategies.

To determine the direction of the model's bifurcation, the center manifold theorem, as outlined in [25], will be employed. The initial step in this process is to calculate the Jacobian at the disease-free equilibrium (2.6).

$$J = \begin{pmatrix}
-\tau - d & 0 & 0 & m_1 & 0 & 0 & 0 & 0 & -\dfrac{K^s\beta_{KG}}{N} \\
0 & -\tau - d - \alpha_1 & 0 & 0 & 0 & 0 & 0 & 0 & \dfrac{K^s\beta_{KG}}{N} \\
0 & \alpha_1 & -\tau - \gamma_1 - d & 0 & 0 & 0 & 0 & 0 & 0 \\
0 & 0 & \gamma_1 & -\tau - m_1 - d & 0 & 0 & 0 & 0 & 0 \\
\tau & 0 & 0 & 0 & -d & 0 & 0 & m_2 & -\dfrac{A^s\beta_{AG}}{N} \\
0 & \tau & 0 & 0 & 0 & -d - \alpha_2 & 0 & 0 & \dfrac{A^s\beta_{AG}}{N} \\
0 & 0 & \tau & 0 & 0 & \alpha_2 & -\gamma_2 - d & 0 & 0 \\
0 & 0 & 0 & \tau & 0 & 0 & \gamma_2 & -m_2 - d & 0 \\
0 & 0 & 0 & 0 & \dfrac{\beta}{N} & \dfrac{\beta}{N} & \dfrac{\beta}{N} & 0 & d_G - b
\end{pmatrix}.$$

Setting $R_0 = 1$ and solving for the parameter β, we obtain

$$\beta = \left[\frac{bA_0^s\alpha_2\beta_{AG}}{N^2(\alpha_2+d)(d+\gamma_2)d_G} + \frac{bA_0^s\beta_{AG}}{N^2(\alpha_2+d)d_G} + \frac{b\alpha_1\beta_{KG}K_0^s\tau}{N^2(d+\gamma_2)(\alpha_1+d+\tau)(d+\gamma_1+\tau)d_G} + \frac{b\alpha_2\beta_{KG}K_0^s\tau}{N^2(\alpha_2+d)(d+\gamma_2)(\alpha_1+d+\tau)d_G} + \frac{b\beta_{KG}K_0^s\tau}{N^2(\alpha_2+d)(\alpha_1+d+\tau)d_G} \right]^{-1}. \tag{2.31}$$

Following an evaluation of the Jacobian at the designated point, denoted by β^*, the right and left eigenvectors, denoted by v and w, respectively, are calculated.

An analysis of the sign of the components of the left eigenvector v allows for the determination of the direction of the model's bifurcation at the critical point $R_0 = 1$.

The left eigenvector v associated with the zero eigenvalue of the Jacobian is expressed in compact form as follows:

$$v = \begin{pmatrix} 0 \\ r_1 \\ \frac{r_1(d+\alpha_2)(\tau+d+\alpha_1)}{\gamma_2\tau+d\tau+\alpha_2\tau+\gamma_1\gamma_2+d\gamma_2+d\gamma_1+\alpha_2\gamma_1+d^2+\alpha_2d+\alpha_1d+\alpha_1\alpha_2} \\ 0 \\ 0 \\ \frac{r_1(\gamma_2+d+\alpha_2)(\tau+d+\alpha_1)(\tau+\gamma_1+d)}{\tau(\gamma_2\tau+d\tau+\alpha_2\tau+\gamma_1\gamma_2+d\gamma_2+d\gamma_1+\alpha_2\gamma_1+d^2+\alpha_2d+\alpha_1d+\alpha_1\alpha_2)} \\ \frac{r_1(d+\alpha_2)(\tau+d+\alpha_1)(\tau+\gamma_1+d)}{\tau(\gamma_2\tau+d\tau+\alpha_2\tau+\gamma_1\gamma_2+d\gamma_2+d\gamma_1+\alpha_2\gamma_1+d^2+\alpha_2d+\alpha_1d+\alpha_1\alpha_2)} \\ 0 \\ \frac{r_1\mu\,\Phi}{d(b-d_G)(\tau+d)(\gamma_2\tau+d\tau+\alpha_2\tau+\gamma_1\gamma_2+d\gamma_2+d\gamma_1+\alpha_2\gamma_1+d^2+\alpha_2d+\alpha_1d+\alpha_1\alpha_2)} \end{pmatrix},$$

where

$$\begin{aligned}\Phi =& \beta_{AG}(\gamma_2\tau^2+d\tau^2+\alpha_2\tau^2+\gamma_1\gamma_2\tau+2d\gamma_2\tau+\alpha_1\gamma_2\tau+d\gamma_1\tau+\alpha_2\gamma_1\tau+2d^2\tau+2\alpha_2d\tau+\alpha_1d\tau+\alpha_1\alpha_2\tau \\ &+d\gamma_1\gamma_2+d^2\gamma_2+\alpha_1d\gamma_2+d^2\gamma_1+\alpha_2d\gamma_1+\alpha_1d\gamma_1+\alpha_1\alpha_2\gamma_1+d^3+\alpha_2d^2+\alpha_1d^2+\alpha_1\alpha_2d) \\ &+\beta_{KG}(d\gamma_2\tau+d^2\tau+\alpha_2d\tau+d\gamma_1\gamma_2+d^2\gamma_2+d^2\gamma_1+\alpha_2d\gamma_1+d^3+\alpha_2d^2+\alpha_1\alpha_2d).\end{aligned}$$

Once the left eigenvector v has been obtained, the right eigenvector w is determined, corresponding to the same zero eigenvalue of the Jacobian matrix evaluated at β^*. This vector satisfies the relation $w^\top J(\beta^*) = 0$ and is normalized so that $w^\top v = 1$. Its general compact form is expressed as

$$w = \begin{pmatrix} r_1 \\ -\frac{r_1(\tau+\gamma_1+d)(\tau+m_1+d)}{\tau^2+m_1\tau+\gamma_1\tau+2d\tau+\alpha_1\tau+\gamma_1m_1+dm_1+\alpha_1m_1+d\gamma_1+\alpha_1\gamma_1+d^2+\alpha_1d} \\ -\frac{r_1\alpha_1(\tau+m_1+d)}{\tau^2+m_1\tau+\gamma_1\tau+2d\tau+\alpha_1\tau+\gamma_1m_1+dm_1+\alpha_1m_1+d\gamma_1+\alpha_1\gamma_1+d^2+\alpha_1d} \\ -\frac{r_1\alpha_1\gamma_1}{\tau^2+m_1\tau+\gamma_1\tau+2d\tau+\alpha_1\tau+\gamma_1m_1+dm_1+\alpha_1m_1+d\gamma_1+\alpha_1\gamma_1+d^2+\alpha_1d} \\ \frac{r_1\tau\Psi}{\beta_{KG}d(d+\alpha_2)(\gamma_2+d)(m_2+d)(\tau^2+m_1\tau+\gamma_1\tau+2d\tau+\alpha_1\tau+\gamma_1m_1+dm_1+\alpha_1m_1+d\gamma_1+\alpha_1\gamma_1+d^2+\alpha_1d)} \\ -\frac{r_1\tau(\tau+\gamma_1+d)(\tau+m_1+d)(\beta_{AG}\tau+\beta_{KG}d+\alpha_1\beta_{AG})}{\beta_{KG}d(d+\alpha_2)(\tau^2+m_1\tau+\gamma_1\tau+2d\tau+\alpha_1\tau+\gamma_1m_1+dm_1+\alpha_1m_1+d\gamma_1+\alpha_1\gamma_1+d^2+\alpha_1d)} \\ -\frac{r_1\tau(\tau+m_1+d)\Xi}{\beta_{KG}d(d+\alpha_2)(\gamma_2+d)(\tau^2+m_1\tau+\gamma_1\tau+2d\tau+\alpha_1\tau+\gamma_1m_1+dm_1+\alpha_1m_1+d\gamma_1+\alpha_1\gamma_1+d^2+\alpha_1d)} \\ -\frac{r_1\tau\Omega}{\beta_{KG}d(d+\alpha_2)(\gamma_2+d)(m_2+d)(\tau^2+m_1\tau+\gamma_1\tau+2d\tau+\alpha_1\tau+\gamma_1m_1+dm_1+\alpha_1m_1+d\gamma_1+\alpha_1\gamma_1+d^2+\alpha_1d)} \\ -\frac{r_1(\tau+d)(\tau+d+\alpha_1)(\tau+\gamma_1+d)(\tau+m_1+d)}{\beta_{KG}\mu(\tau^2+m_1\tau+\gamma_1\tau+2d\tau+\alpha_1\tau+\gamma_1m_1+dm_1+\alpha_1m_1+d\gamma_1+\alpha_1\gamma_1+d^2+\alpha_1d)} \end{pmatrix}.$$

The term Ω denotes the common denominator, which incorporates a series of parameters, namely $\tau, \gamma_1, \gamma_2, m_1, m_2, \alpha_1, \alpha_2, d, \beta_{KG}, \beta_{AG}$, and Ψ, which collectively represent the polynomial numerator of the fifth component of the given vector. This factor Ω is analogous to Φ in the eigenvector v but for the right eigenvector w.

According to the center manifold theorem (see in the Appendix section), to determine the direction of the bifurcation, it is necessary to calculate the signs of the coefficients a and b of the normal forms associated with the system (2.1). In this case, the coefficient b is always positive, and a is negative. Therefore, the model (2.1) exhibits a forward bifurcation at $R_0 = 1$.

2.6. Global stability

Theorem 4 (Global stability of the disease-free equilibrium)**.** *Assume that $d_G > b$. If the basic reproductive number satisfies $R_0 \leq 1$, then the disease-free equilibrium*

$$x^* = \left(\frac{\mu N}{d+\tau}, 0, 0, 0, \frac{\tau\mu N}{d(d+\tau)}, 0, 0, 0, 0\right)$$

of system (2.1) is globally asymptotically stable in the positively invariant region Ω.

Proof. Consider the Lyapunov function

$$V = c_1Ke + c_2Ki + c_3Ae + c_4Ai + c_5G, \tag{2.32}$$

where the positive coefficients c_i are defined as

$$\begin{aligned} c_2 &= \frac{c_1\alpha_1}{d+\tau+\gamma_1}, \\ c_3 &= \frac{c_1\tau}{d+\alpha_2}, \\ c_4 &= \frac{c_3\alpha_2}{d+\gamma_2}, \\ c_5 &= \frac{c_4(d+\gamma_2)}{\beta/N}. \end{aligned} \tag{2.33}$$

Differentiating (2.32) along the solutions of system (2.1) and rearranging terms, we obtain

$$\begin{aligned}\dot{V} = {} & Ke\Big[c_2\alpha_1 + c_3\tau - c_1(d+\tau+\alpha_1)\Big] \\ & + Ki\Big[c_4\tau - c_2(d+\tau+\gamma_1)\Big] \\ & + Ae\Big[c_4\alpha_2 + c_5\frac{\beta}{N} - c_3(d+\alpha_2)\Big] \\ & + Ai\Big[c_5\frac{\beta}{N} - c_4(d+\gamma_2)\Big] \\ & + G\Big[c_1\frac{\beta_K Ks}{N} + c_3\frac{\beta_A As}{N} + c_5(b-d_G)\Big]. \end{aligned} \tag{2.34}$$

By construction of the coefficients (2.33), there exist constants $\kappa_i > 0$, $i = 1, 2, 3$, such that

$$\dot{V} = -\kappa_1 Ke - \kappa_2 Ki - \kappa_3 Ae + G\Big[c_1\frac{\beta_K Ks}{N} + c_3\frac{\beta_A As}{N} + c_5(b-d_G)\Big]. \tag{2.35}$$

Evaluating the susceptible compartments at the disease-free equilibrium,

$$Ks^* = \frac{\mu N}{d+\tau}, \qquad As^* = \frac{\tau\mu N}{d(d+\tau)}, \tag{2.36}$$

the remaining term involving G becomes

$$G\left[\frac{c_1\beta_K}{N}Ks^* + \frac{c_3\beta_A}{N}As^* + c_5(b-d_G)\right]. \tag{2.37}$$

Substituting (2.36) into (2.37), we obtain

$$\begin{aligned} & G\left[\frac{c_1\beta_K}{N}\frac{\mu N}{d+\tau} + \frac{c_3\beta_A}{N}\frac{\tau\mu N}{d(d+\tau)} + c_5(b-d_G)\right] \\ & = G\left[\frac{c_1\mu\beta_K}{d+\tau} + \frac{c_3\tau\mu\beta_A}{d(d+\tau)} + c_5(b-d_G)\right]. \end{aligned} \tag{2.38}$$

Next, we express the first two terms in (2.38) in terms of c_5. Using again (2.33), we obtain

$$c_1 = c_5\,\frac{\beta}{N}\frac{(d+\alpha_2)(d+\gamma_2)}{\tau\alpha_2}, \qquad c_3 = c_5\,\frac{\beta}{N}\frac{d+\gamma_2}{\alpha_2}. \tag{2.39}$$

Substituting (2.39) into (2.38) yields

$$\begin{aligned} & c_5 G\left[\frac{\beta}{N}\frac{(d+\alpha_2)(d+\gamma_2)}{\tau\alpha_2}\frac{\mu\beta_K}{d+\tau} + \frac{\beta}{N}\frac{d+\gamma_2}{\alpha_2}\frac{\tau\mu\beta_A}{d(d+\tau)} - (d_G-b)\right] \\ & = (d_G-b)c_5\,(R_0-1)\,G. \end{aligned} \tag{2.40}$$

The fraction appearing in (2.40) coincides exactly with the basic reproductive number R_0, previously obtained by the next-generation matrix method. Hence,

$$\dot{V} \le (d_G-b)c_5(R_0-1)G. \tag{2.41}$$

Because $d_G > b$, and $R_0 \leq 1$, it follows from (2.41) that $\dot{V} \leq 0$ in Ω, and

$$\dot{V} = 0 \quad \Longleftrightarrow \quad Ke = Ki = Ae = Ai = G = 0.$$

The largest invariant set contained in $\{\dot{V} = 0\}$ is the disease-free equilibrium x^*. By LaSalle's invariance principle, x^* is globally asymptotically stable in Ω.

Remark. *The condition $d_G > b$ guarantees that the environmental pathogen population decays in the absence of new infections, which is essential for global stability of the disease-free equilibrium.*

2.7. Local stability and forward bifurcation

The local dynamics of system (2.1) near the disease-free equilibrium are governed by the spectral properties of the linearized system at the critical threshold $R_0 = 1$. At this value, the Jacobian matrix has a simple zero eigenvalue, and all remaining eigenvalues have negative real parts. As a consequence, linearization alone is not sufficient to characterize the local behavior of solutions.

According to the center manifold theorem (see the Appendix Material), the qualitative dynamics of system (2.1) in a neighborhood of the disease-free equilibrium at $R_0 = 1$ are completely determined by the flow restricted to a one-dimensional center manifold. In particular, the stability and bifurcation properties of the equilibrium can be inferred from the reduced normal form

$$\dot{u} = au^2 + b\mu u + O(|u|^3),$$

where u represents the coordinate on the center manifold, $\mu = R_0 - 1$ is the bifurcation parameter, and the coefficients a and b depend on the model parameters.

The sign of the coefficient b determines the direction in which equilibria bifurcate from the disease-free equilibrium, and the sign of a determines their local stability. For the present model, explicit calculations show that $b > 0$ for all admissible parameter values, whereas $a < 0$. Therefore, when R_0 crosses the critical value $R_0 = 1$, a branch of locally asymptotically stable endemic equilibria emerges for $R_0 > 1$, but the disease-free equilibrium loses stability.

This behavior corresponds to a forward (supercritical) bifurcation, which implies that the transition from disease extinction to persistence occurs smoothly as R_0 increases through unity.

Theorem 5 (Forward bifurcation at the disease-free equilibrium)**.** *Let R_0 denote the basic reproductive number associated with system (2.1). Assume that all model parameters are positive. Then, at $R_0 = 1$, the disease-free equilibrium of system (2.1) undergoes a forward (supercritical) bifurcation. In particular, the disease-free equilibrium is locally asymptotically stable for $R_0 < 1$ and unstable for $R_0 > 1$, and a unique locally asymptotically stable endemic equilibrium exists for $R_0 > 1$ sufficiently close to one.*

3. Results

To illustrate the dynamics of CE transmission, the system of ordinary differential equations described in Eq (2.1) was numerically solved using the ode45 function in MATLAB (version R2022a [26]). This integrator, based on the explicit Runge-Kutta method of order 4(5) with variable step size, allows for efficient control of local error by automatically adjusting the step size according

to the variability of the solution. The numerical simulations were performed using the values documented in Tables 1 and 2, which correspond to the parameters and initial data, respectively. To illustrate the phenomenon of adults who are inadvertently infected during childhood due to undetected disease, a simulation of its dynamics over a 20-year period was performed.

3.1. Impact of the infestation rate on the number of infected individuals

In this section, we will present simulations for model (2.1) using the parameter values available in the literature (see Table 1). The initial values are presented in Table 2.

As illustrated in Figure 2(a),(b), a decrease in the concentration of *E. granulosus s.l.* eggs leads to a concurrent decrease in the number of infected individuals, affecting both children and adults. Figure 2(c),(d) illustrate the impact of an increase in the concentration of *E. granulosus s.l.* eggs on the number of human subjects, both children and adults, infected with CE.

Table 1. Definitions and values of epidemiological parameters (unit: yr^{-1}).

Parameter	Description	Value	Range	Reference
μ	Human birth rate	0.0141	0.0141–0.4161	[16–20]
d	Human death rate	0.0141	0.0141–0.4161	[16–20]
β_{KG}	Transmission rate to human juveniles	0.0323	1.0×10^{-11}–0.0430	[16, 17, 19, 20]
β_{AG}	Transmission rate to human adults	0.0323	1.0×10^{-11}–0.0430	[16, 17, 19, 20]
β	*E. granulosus* infestation rate	18.0328	0–1.0×10^2	[11]
d_G	Parasite egg mortality rate	10.4200	–	[17]
b	Released rate from infected dog	9.7000	–	[17]
α_1	Rate at which exposed juveniles become infected	0.0703	0.0693–0.0714	[16, 18, 20]
α_2	Rate at which exposed adults become infected	0.0703	0.0693–0.0714	[16, 18, 20]
γ_1	Treatment rate (juveniles)	0.5000	0.0500–0.5000	[27]
γ_2	Treatment rate (adults)	0.5000	0.0500–0.5000	[27]
τ	Average time from child to adult ($1/\tau$)	0.0667	–	Assumed
m_1	Loss of immunity rate (juveniles)	0.5000	–	Assumed
m_2	Loss of immunity rate (adults)	0.5000	–	Assumed

Table 2. Initial conditions.

Variable	Description	Initial value
K^s	Susceptible children	27,167
K^e	Exposed children	310
K^i	Infected children	0
K^r	Recovered children	0
A^s	Susceptible adults	27,232
A^e	Exposed adults	100
A^i	Infected adults	0
A^r	Recovered adults	0
G	*E. granulosus s.l.* eggs	1.4400×10^7

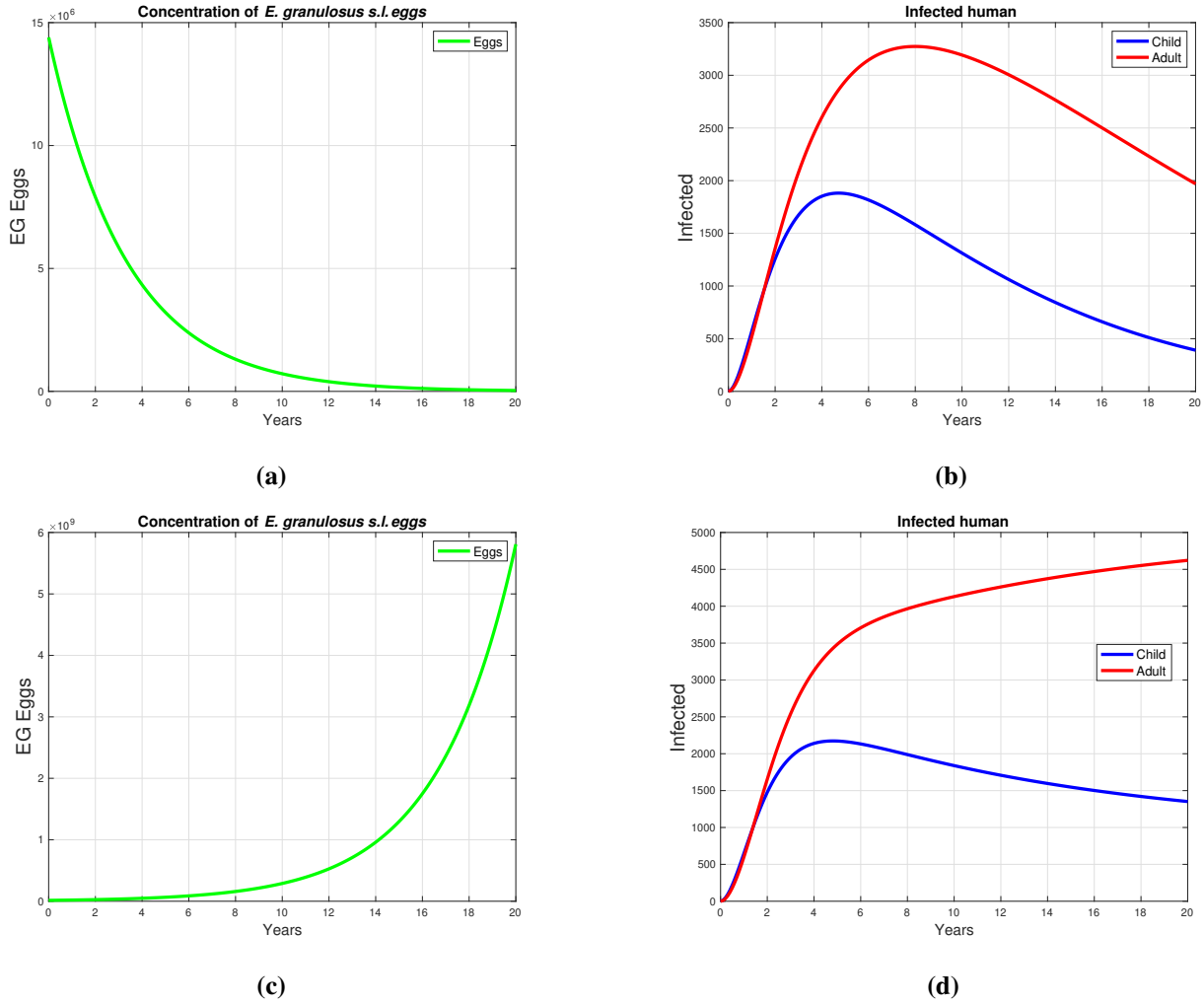

Figure 2. The concentration of *E. granulosus s.l.* eggs affects the prevalence of CE infection in children and adults.

3.2. Sensitivity analysis

In order to quantify the influence of certain parameters on the basic reproductive number, R_0, a global sensitivity analysis was performed. This analysis was based on Sobol indices [28] and was carried out using Python's SALib library. The problem was defined through the establishment of fixed values for the parameters b, d_G, m_1, m_2, τ, and N. In addition, ranges of variation were determined for the nine parameters of interest: α_1, α_2, β, β_{KG}, β_{AG}, d, γ_1, γ_2, and μ. We then employed Saltelli's sampling method, which extends the Sobol sequence to ensure efficient and uniform exploration of the parameter space, generating 10,000 samples per parameter with second-order interaction. For each set of parameters, the function defining R_0 was evaluated, and the first-order and total-order Sobol indices were calculated from the results obtained.

Let us analyze the sensitivity indices shown in Table 3 and Figure 3. The most influential parameters on R_0 are β, β_{AG}, and d, and parameters α_1, α_2, γ_1, and μ are noninfluential, as their total indices are

negligible. β and β_{AG} are controllable parameters. In particular, this suggests that if the infestation rate could be reduced, the variability in the basic reproductive number of *E. granulosus s.l.* infection in humans would also be reduced. The sum of the first-order effects is approximately 0.9, indicating that not all variance in R_0 is explained by the parameters independently. That is, there are interactions between them. The total sum of the indices is approximately 1.1, which indicates the presence of interactions, as it captures both the individual and combined effects of the parameters. This discrepancy between the sums provides a quantitative illustration of the interactions between the parameters of R_0, with the magnitude of the difference indicating the magnitude of these interactions.

Table 3. First-order and total-effect sensitivity indices obtained with the method of Saltelli.

Parameter	First-order indices	Total-order indices
α_1	0.0000	0.0000
α_2	-0.0000	0.0000
β	0.3590	0.4290
β_{KG}	0.0010	0.0020
β_{AG}	0.2990	0.3620
d	0.2400	0.3000
γ_1	-0.0000	0.0000
γ_2	0.0040	0.0060
μ	0.0000	0.0000

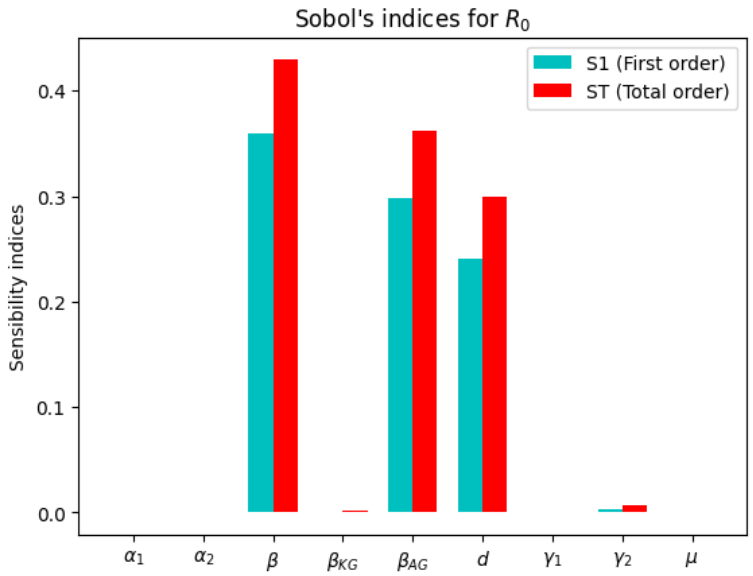

Figure 3. First-order and total Sobol indices for 9 parameters of the basic reproductive number of model (2.1).

4. Discussion

The infestation index serves as the primary metric for establishing risk levels and defining control zones for CE. Consequently, findings from laboratory analyses of environmental samples, including dog feces, soil, surface water, and fur [1–5, 9–11], are instrumental in calculating this index. The model incorporates the infestation rate, β, as a key parameter, based on the hypothesis that establishing temporal regularity in environmental monitoring is feasible for detecting viable *E. granulosus s.l.* eggs.

As established in previous studies [23–25], analyzing the bifurcation type in mathematical models for infectious disease dynamics is of paramount importance, as it determines the feasibility of eradication strategies. While this mathematical model does not directly incorporate the specific behaviors of dogs and sheep, this strategic simplification enables a rigorous analysis of the bifurcation type. The identification of a forward bifurcation indicates that the disease can potentially be eradicated through the implementation of suitable control measures.

Previous research [12–15] developed mathematical models to understand CE transmission from infected animals to humans, with sensitivity analyses identifying transmission rates as highly influential parameters for the basic reproductive number (R_0). The present sensitivity analysis, utilizing Sobol indices [28], demonstrates that the infestation rate (β) has the greatest impact on R_0. This validates its status as a primary target for public health interventions. This parameter, which is based on the environmental infestation index (EII) obtained through coproparasitological diagnoses in dogs, stands as a critical factor in the reemergence of the disease [8].

The incorporation of the β parameter into the extended SEIR model serves as a proof-of-concept. It demonstrates that periodic sampling (e.g., semiannual) provides valuable data for reducing R_0 by minimizing the environmental burden of viable eggs. Specifically, implementing strict regulations on sheep slaughter and the disposal of infected viscera, common practices in endemic sheep-farming areas, results in lower infestation rates, thereby facilitating disease eradication.

The predictive performance of the model, based on the integration of epidemiological data, improves the surveillance of cystic echinococcosis. The implementation of periodic coprological diagnostics instead of eventual sampling provides a robust basis for estimating the infestation rate, a central parameter for projecting the human disease burden. In this way, the model improves the efficient allocation of resources, guiding parasitic control strategies (such as those as discussed in [29]) in dogs, vaccination of intermediate hosts, and early detection in humans by serological and ultrasonographic techniques.

In establishing a baseline for the disease in dogs, the EII allows for the definition of risk levels and priority control areas. Calculating this index requires the detection of *E. granulosus s.l.* in the environment, typically through the analysis of representative fecal samples from dogs within specific epidemiological units. However, these analyses are currently not conducted on a regular basis. Consequently, a key limitation of the model is its reliance on the environmental infestation rate, as the practical data required for its determination are not routinely available in many study areas.

5. Conclusions

In this study, a mathematical model was developed and analyzed as a proof of concept with the aim of describing the dynamics of transmission of the *E. granulosus s.l.* parasite to humans. The

model incorporates the infestation rate. Assuming constant disease transmission rates, the next-generation matrix was implemented to calculate the basic reproductive number, R_0. A sensitivity analysis was conducted, revealing that the disease transmission rate and infestation rate are the parameters that most influence the variability of R_0. Specifically, 29.90% of the variance of R_0 in the model is directly explained by the parameter β_{AG}, and 35.90% is explained by the parameter β, revealing that a reduction in the parameters, β and β_{AG} would lead to a decrease in human infections by *E. granulosus s.l.* A viable strategy for β_{AG} is to educate the rural population to avoid close contact with dogs in sheep farming environments, thereby minimizing zoonotic exposure. β could be reduced by improving sheep slaughtering practices and the safe disposal of viscera, preventing dogs from feeding on it, and reducing the resulting environmental burden of parasite eggs. Consequently, these findings underscore the importance of integrated One Health interventions that combine community education and dog reservoir control to interrupt the transmission cycle in endemic regions. The calculation of the proportion of variance contributed by individual parameters and their interactions with other parameters was determined to be 36.2% and 42.9%, respectively. In the present study, a bifurcation analysis of the model was carried out, through which it was determined that the bifurcation is forward. Therefore, it has been established that a clear threshold for the eradication of the disease is one that meets the condition $R_0 < 1$. Consequently, it has been determined that a strategy aimed at reducing β_{AG} and β could potentially lead to a decrease in human infections. In this study, it has been observed that, by incorporating the infestation rate into the mathematical model, human behavior can be characterized as responsible for perpetuating the parasite's life cycle. In addition, the simulations have depicted a clear association between the variations in the availability of *E. granulosus s.l.*, and the number of infected humans.

Acknowledgments

This work was partially supported by the UNAM Postdoctoral Program (POSDOC). The authors also would like to thank the Center for Research in Mathematics (CIMAT) and the SEITCHI program for the doctoral fellowship. Additionally, we express our gratitude to Universidad de Magallanes (Chile), Universidad El Bosque (Colombia), and Universidad de los Llanos (Colombia) for the institutional support and facilities provided to the authors during this research.

Conflict of interest

The authors declare no conflicts of interest.

Use of AI tools declaration

During the preparation of this work, the authors used Perplexity (GPT-5.1) to assist with language editing and improvement of the English text. After using this tool, the authors carefully reviewed and edited all content and take full responsibility for the final version of the manuscript.

References

1. T. Mohammed, S. L. Ezzat, H. S. Abdullah, S. J. Qadir, A. K. Hamad, S. A. Faraj, et al., *E*chinococcus granulosus in environmental samples: A cross-sectional molecular study, *Barw Med. J.*, **3** (2025), 9–14. https://doi.org/10.58742/bmj.vi.200
2. G. Acosta-Jamett, F. Tamarozzi, N. Castro, S. J. Santivanez, R. E. Laurente, C. Mazzi, et al., Community risk of environmental-borne cystic echinococcosis transmission in South America: Results from the multistep cross-sectional and case-control PERITAS study, *PLoS Negl. Trop. Dis.*, **19** (2025), 1–14. https://doi.org/10.1371/journal.pntd.0013382
3. E. Serra, G. Masu, V. Chisu, S. Cappai, G. Masala, F. Loi, et al., Environmental contamination by Echinococcus spp. eggs as a risk for human health in educational farms of Sardinia, Italy, *Vet. Sci.*, **9** (2022), 143. https://doi.org/10.3390/vetsci9030143
4. C. A. Alvarez, A. Mathis, P. Deplazes, Assessing the contamination of food and the environment with Taenia and Echinococcus eggs and their zoonotic transmission, *Curr. Clin. Microbiol. Rep.*, **5** (2018), 154–163. https://doi.org/10.1007/s40588-018-0091-0
5. K. Federer, M. T. Armua-Fernandez, F. Gori, S. Hoby, C. Wenker, P. Deplazes, Detection of taeniid (Taenia spp., Echinococcus spp.) eggs contaminating vegetables and fruits sold in European markets and the risk for metacestode infections in captive primates, *Int. J. Parasitol.: Parasites Wildl.*, **5** (2016), 249–253. https://doi.org/10.1016/j.ijppaw.2016.07.002
6. Z. Valieva, N. Sarsembaeva, A. Valdovska, A. E. Ussenbayev, Impact of Echinococcosis on quality of sheep meat in the south eastern Kazakhstan, *Asian-Australas. J. Anim. Sci.*, **27** (2014), 391–397. https://doi.org/10.5713/ajas.2013.13386
7. E. Larrieu, G. Mujica, C. G. Gauci, K. Vizcaychipi, M. Seleiman, E. Herrero, et al., Pilot field trial of the EG95 vaccine against ovine cystic Echinococcosis in Rio Negro, Argentina: Second study of impact, *PLoS Negl. Trop. Dis.*, **9** (2015), 1–10. https://doi.org/10.1371/journal.pntd.0004134
8. Manual para el diagnóstico, tratamiento, prevención y control de la Hidatidosis en Chile, 2015. Available from: https://diprece.minsal.cl/wrdprss_minsal/wp-content/uploads/2016/02/Manual-Hidatidosis.pdf.
9. M. Reza, S. Mohammad, M. Ali, S. Nasibi, S. Shamsaddini, F. Mollaee, et al., Surface water contamination with *E*chinococcus granulosus eggs in southeast of iran: Significance and public health implications, *J. Water Health*, **23** (2025), 981–990. https://doi.org/10.2166/wh.2025.244
10. R. Barosi, G. Umhang, Presence of Echinococcus eggs in the environment and food: A review of current data and future prospects, *Parasitology*, **13** (2024), 1416–1431. https://doi.org/10.1017/s0031182024000945
11. J. F. Alvarez, R. Ruiz, J. Ríos, C. A. Alvarez, Molecular detection of *E*chinococcus granulosus sensu stricto in environmental dog faecal samples from the Magallanes region, Patagonia, Chile, *Parasitologia*, **1** (2021), 238–246. https://doi.org/10.3390/parasitologia1040025
12. R. Lagos, J. P. Gutiérrez-Jara, B. Cancino-Faure, L. Y. Lara-Díaz, Sensitivity analysis of a mathematical model for the transmission of cystic echinococcosis, *J. Phys. Conf. Ser.*, **3117** (2025), 012011. https://doi.org/10.1088/1742-6596/3117/1/012011

13. R. Lagos, J. P. Gutiérrez-Jara, B. Cancino-Faure, L. Y. Lara-Díaz, A. González-Galeano, Breaking the cycle of Echinococcosis: A mathematical modeling approach, *Trop. Med. Infect. Dis.*, **10** (2025), 101. https://doi.org/10.3390/tropicalmed10040101

14. R. Lagos, J. P. Gutiérrez-Jara, B. Cancino-Faure, L. Y. Lara-Díaz, A. Coronel, The role of host mobility in the transmission and spread of *E*chinococcus granulosus: A Chile-based mathematical modeling approach *PLoS Negl. Trop. Dis.*, **19** (2025), e0012948. https://doi.org/10.1371/journal.pntd.0012948

15. J. A. M. Atkinson, G. M. Williams, L. Yakob, A. C. A. Clements, T. S. Barnes, D. McManus, et al., Synthesising 30 years of mathematical modelling of Echinococcus transmission, *PLoS Negl. Trop. Dis.*, **7** (2013), e2386. https://doi.org/10.1371/journal.pntd.0002386

16. G. B. Birhan, J. M. W. Munganga, A. S. Hassan, Mathematical modeling of Echinococcosis in humans, dogs, and sheep, *J. Appl. Math.*, **2020** (2020), 8482696. https://doi.org/10.1155/2020/8482696

17. K. Wang, X. Zhang, Z. Jin, H. Ma, Z. Teng, L. Wang, Modeling and analysis of the transmission of Echinococcosis with application to Xinjiang Uygur autonomous region of China, *J. Theor. Biol.*, **333** (2013), 78–90. https://doi.org/10.1016/j.jtbi.2013.04.020

18. C. S. Chacha, M. A. Stephano, J. I. Irunde, J. A. Mwasunda, Cystic echinococcosis dynamics in dogs, humans and cattle: Deterministic and stochastic modeling, *Results Phys.*, **51** (2023), 106697. https://doi.org/10.1016/j.rinp.2023.106697

19. L. Wu, B. Song, W. Du, J. Lou, Mathematical modelling and control of echinococcus in Qinghai province, China, *Math. Biosci. Eng.*, **10** (2013), 425–444. https://doi.org/10.3934/mbe.2013.10.425

20. B. Getachew, J. M. W. Munganga, A. S. Hassan, Mathematical modelling of echinococcosis in human, dogs and sheep with intervention, *J. Biol. Dyn.*, **16** (2022), 439–463. https://doi.org/10.1080/17513758.2022.2081368

21. A. González-Galeano, I. Barradas, J. Villavicencio, Beyond R0: Exploring new approaches, *Rev. Modelamiento Mat. Sistemas Biol.*, **3** (2023), e23R08. https://doi.org/10.58560/rmmsb.v03.n02.023.09

22. P. van den Driessche, J. Watmough, Reproduction numbers and sub-threshold endemic equilibria for compartmental models of disease transmission, *Math. Biosci.*, **180** (2002), 29–48. https://doi.org/10.1016/S0025-5564(02)00108-6

23. W. Wang, Backward bifurcation of an epidemic model with treatment, *Math. Biosci.*, **201** (2006), 58–71. https://doi.org/10.1016/j.mbs.2005.12.022

24. J. G. Villavicencio, J. I. Barradas, J. C. Hernández, A basic backward Bifurcation model in epidemiology, *Appl. Math. Sci.*, **7** (2013), 5327–5340. https://doi.org/10.12988/AMS.2013.36324

25. C. Castillo-Chavez, B. Song, Dynamical models of tuberculosis and their applications, *Math. Biosci. Eng.*, **1** (2004), 361–404. https://doi.org/10.3934/mbe.2004.1.361

26. The MathWorks, MATLAB and simulink for engineered systems, 2023. Available from: https://www.mathworks.com.

27. B. J. Bogitsh, C. E. Carter, T. N. Oeltmann, *Human Parasitology*, 5^{th} edition, Academic Press, 2019. https://doi.org/10.1016/C2016-0-00382-0

28. A. Saltelli, M. Ratto, T. Andres, F. Campolongo, J. Cariboni, D. Gatelli, et al., *Global Sensitivity Analysis: The Primer*, John Wiley & Sons, Chichester, 2008. https://doi.org/10.1002/9780470725184

29. C. Alvarez, F. Fredes, M. Torres, G. Acosta-Jamett, J. Alvarez, C. Pavletic, et al., First meeting "Cystic echinococcosis in Chile, update in alternatives for control and diagnostics in animals and humans", *Parasites Vectors*, **9** (2016), 502. https://doi.org/10.1186/s13071-016-1792-y

A. Appendix

Consider a general system of ODEs with a parameter φ,

$$\frac{dx}{dt} = f(x, \varphi), \tag{A.1}$$

$f : \mathbb{R}^n \times \mathbb{R}$, $f \in C^2(\mathbb{R}^n \times \mathbb{R})$.

Without a loss of generality, it is assumed that 0 is an equilibrium for system (A.1) for all values of the parameter φ, that is,

$$f(0, \varphi) \equiv 0 \quad \text{for all } \varphi. \tag{A.2}$$

Theorem 6 (Center manifold theorem)**.** *Assume*

A1: $A = D_x f(0,0) = \left(\partial f_i x_j(0,0)\right)$ *is the linearization matrix of system* (A.1) *around the equilibrium* 0 *with* φ *evaluated at* 0*. Zero is a simple eigenvalue of A, and all other eigenvalues of A have negative real parts;*

A2: Matrix A has a nonnegative right eigenvector w and a left eigenvector v corresponding to the zero eigenvalue.

Let f_k *be the kth component of* f *and*

$$a = \sum_{k,i,j=1}^{n} v_k w_i w_j \frac{\partial^2 f_k}{\partial x_i \partial x_j}(0,0), \tag{A.3}$$

$$b = \sum_{k,i=1}^{n} v_k w_i \frac{\partial^2 f_k}{\partial x_i \partial \varphi}(0,0). \tag{A.4}$$

The local dynamics of (A.1) *around* 0 *are totally determined by a and b.*

1) $a > 0$, $b > 0$
   When $\varphi < 0$ *with* $|\varphi| << 1$, 0 *is locally asymptotically stable, and there exists a positive unstable equilibrium; when* $0 < \varphi << 1$, 0 *is unstable and there exists a negative and locally asymptotically stable equilibrium;*
2) $a < 0$, $b < 0$
   When $\varphi < 0$ *with* $|\varphi| << 1$, 0 *is unstable; when* $0 < \varphi << 1$, 0 *is locally asymptotically stable, and there exists a positive unstable equilibrium;*

3) $a > 0$, $b < 0$
When $\varphi < 0$ *with* $|\varphi| << 1$, 0 *is unstable, and there exists a locally asymptotically stable negative equilibrium; when* $0 < \varphi << 1$, 0 *is stable, and a positive unstable equilibrium appears;*
4) $a < 0$, $b > 0$
When φ *changes from negative to positive,* 0 *changes its stability from stable to unstable. Correspondingly, a negative unstable equilibrium becomes positive and locally asymptotically stable.*

AIMS Press